The oxidation of the novel lignocellulosic biofuel γ-valerolactone in a low pressure flame

Alena Sudholt, Rupali Tripathi, Daniel A. Mayer, Pierre-Alexandre Glaude, Frédérique Battin-Leclerc, Heinz Pitsch

*Title Page

The oxidation of the novel lignocellulosic biofuel γ-valerolactone in a low pressure flame

Alena Sudholt[1], Rupali Tripathi[1], Daniel Mayer[1], Pierre-Alexandre Glaude[2], Frédérique Battin-Leclerc[2], Heinz Pitsch[1]

[1] Institute for Combustion Technology, RWTH Aachen University, 52056 Aachen, Germany

[2] Laboratoire Réactions et Génie des Procédés, CNRS, Université de Lorraine, 1 Rue Grandville, 54001 Nancy Cedex, France

Corresponding author:
Alena Sudholt
Institute for Combustion Technology, RWTH Aachen University
Templergraben 64, 52056 Aachen, Germany
Phone: +49/241/80-94613, Fax: +49/241/80-92923
Email address: a.sudholt@itv.rwth-aachen.de

- Preferred colloquium topics: Reaction Kinetics
- Keywords: γ-Valerolactone, Low pressure flame, Kinetic modeling, Species measurements
- Short running title: A γ-valerolactone low pressure flame
- Word count (using method 2): **6 full pages $\times$ 900 word/page and 150mm*2.2 = 5730**

The oxidation of the novel lignocellulosic biofuel γ-valerolactone in a low pressure flame

Alena Sudholt[a,*], Rupali Tripathi[a], Daniel Mayer[a], Pierre-Alexandre Glaude[b], Frédérique Battin-Leclerc[b], Heinz Pitsch[a]

[a] *Institute for Combustion Technology, Templergraben 64, RWTH Aachen University, 52056 Aachen, Germany*
[b] *Laboratoire Réactions et Génie des Procédés, CNRS, Université de Lorraine, 1 Rue Grandville, 54001 Nancy Cedex, France*

Abstract

A first oxidation study of the novel lignocellulosic biofuel γ-valerolactone (GVL) has been performed in a low pressure premixed flat flame. A stoichiometric GVL/methane flame was investigated experimentally and numerically at a pressure of 50 Torr. The measurements include flame temperatures and species concentrations. Species profiles from online gas chromatography measurements are presented for about 40 species including oxygen, hydrogen, argon, carbon monoxide, carbon dioxide, water, hydrocarbon, and oxygenated species with separated isomers. The recent kinetic model for GVL pyrolysis of De Bruycker et al. (Comb. Flame 2015, accepted) was extended for oxidation and the resulting model shows good agreement with the experimental flame data. A reaction pathway analysis was performed, which elucidates the fuel specific oxidation pathways of GVL at the investigated conditions. Additionally, an enthalpy analysis of the flame was performed highlighting

*Corresponding author:
Email address: a.sudholt@itv.rwth-aachen.de (Alena Sudholt)

the consistency of the different measurement techniques.

Keywords: γ-Valerolactone, Low pressure flame, Kinetic modeling, Species measurements

1. Introduction

In the search for novel bio-fuels from non-edible feedstocks, γ-valerolactone (a cyclic ester, $C_5H_8O_2$) has been identified as a safe and sustainable bio-derived molecule [1]. γ-valerolactone (GVL) has since been discussed as a bio-based platform molecule, a green solvent, a potential bio-fuel, and a fuel additive for gasoline or diesel fuels [2–5]. It is not prone to dangerous peroxide formations which increases its applicability for large scale use [1] and enables easy storage and handling. The fact that GVL, contrary to ethanol, does not form an azeotrope with water decreases the energy need of its production process. Being a promising bio-derived replacement for petroleum-based industries, many efforts in the development and improvement of GVL production pathways from biomass have been undertaken. Its production pathways from cellulose via levulinic acid are well studied, and significant improvements in yield and selectivity have been reached in the catalytic conversion processes [6]. Further, novel production pathways from lignocellulosic biomass to GVL have been revealed [2, 3, 5, 7], which establishes GVL as a second generation bio-fuel. Besides presenting pure GVL as a promising green solvent, Horváth et al. [1] investigated physical and chemical properties of gasoline/GVL blends in comparison with gasoline/ethanol blends relevant for transportation fuel applications, such as vapor pressure, boiling point, and water/GVL equilibrium curves. Both of these blends had an additive

content of 10 vol% and showed mostly similar behavior. Solely the vapor pressure of the GVL/gasoline blend was lower than that of the ethanol/gasoline blend. Bereczky et al. [4] investigated the influence of blending GVL into diesel and bio-diesel in a four-cylinder, unmodified diesel engine. They found that engine performance and NO_x-emissions remained unchanged, but carbon monoxide, unburned fuel, and soot emissions were significantly reduced. De Bruycker et al. [8] evaluated the decomposition of GVL under pyrolytic conditions at 0.17 MPa and a temperature range of 873 K to 1073 K experimentally and numerically. They found 4-pentenoic acid, C_4-olefins, carbon monoxide, and carbon dioxide to be the major components in the pyrolysis effluent and supported their experimental observations with a detailed quantum kinetic study of the potential energy surface of GVL decomposition. Recently, De Bruycker et al. [9] extended this work and developed a kinetic model for the pyrolysis of GVL. The model consists of 520 species and 3589 reactions. The thermodynamic and kinetic rate data was mostly calculated at CBS-QB3 level of theory and GVL isomerization to 4-pentenoic acid and H-abstraction of the fuel were found to be the major GVL consumption pathways. They further elucidated the relevance of the isomerization reaction with additional experimental studies of GVL pyrolysis in the presence of the radical scavenger toluene. Its character as relatively easily accessible biosolvent induced the development of sustainable GVL production pathways. The availability of production pathways in turn makes it such an interesting candidate for bio-fuel application. However, the kinetics of the oxidation of GVL have not been studied up to now. Hence, a detailed experimental study of the oxidation of GVL is undertaken in a laminar premixed flat flame and

a kinetic model of its high temperature oxidation is proposed. To the best of our knowledge, the oxidation of GVL has not yet been studied and this fundamental experimental investigation and modeling work of GVL is the first of its kind. An additional enthalpy analysis of the flame has been performed based on its measured composition. It is introduced as an approach to evaluate the consistency of flame measurements. The presented work is structured as follows: The burner setup and the species and temperature measurements are illustrated in section two, the development of the kinetic model and the flame simulation setup are highlighted in section three, the results of the experimental and modeling study are presented, compared, and discussed in section four and the enthalpy analysis is presented in section five. The conclusion follows in section six.

2. Low pressure flame experiments

The oxidation behavior of γ-valerolactone is studied experimentally in a stoichiometric premixed flat flame at low pressure. The experimental setup consists of a vertically displaceable McKenna burner located in a vacuum chamber and a quartz glass micro probe with which gas samples are drawn from the flame. The samples are taken online and evaluated with gas chromatographs. Optionally, a high temperature resistant thermocouple can be installed for flame temperature measurements. Note that all species measurements are performed with the thermocouple removed. A brief overview of the experimental setup and procedure is given in the following and a schematic of the setup is shown in Fig. 1. Further experimental details can be found in Refs. [10, 11].

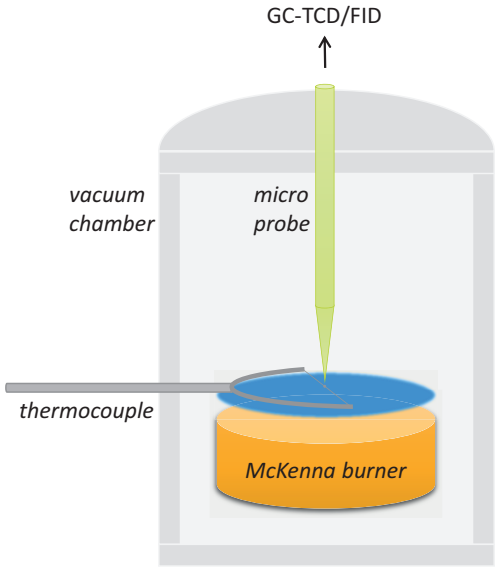

Figure 1: Flat flame burner with micro probe and thermocouple in a vacuum chamber.

It was found that the low vapor pressure of GVL leads to condensation issues in the McKenna burner and that reliable and reproducible measurements of the pure fuel are technically not feasible in this setup. Hence, GVL is investigated as drop-in fuel with methane and an oxygen/argon mixture as oxidizer. The addition of methane to the fuel mainly leads to an increased CH_3 radical mole fraction, therefore no additional cross-reactions are introduced by the blending. The pressure in the vacuum chamber is set to 50 Torr ($\approx$ 6.66 kPa), the diameter of the burner is 0.06 m, its temperature is set to 363 K, and the total volume flow through the burner is 5.47 l_N/min. The reactive mixture is produced with a Bronkhorst vaporizer system consisting of thermal mass flow controllers for all gas flows, a Cori-Tech mini coriolis controller for the liquid, and a CEM (controlled evaporation and mixing) vaporizer unit. The liquid fuel is vaporized with argon and subsequently mixed

ϕ	$X_{\mathrm{CH_4}}$	X_{GVL}	$X_{\mathrm{O_2}}$	X_{Ar}	vfl [$\mathrm{l_N}$/min]
1.042	0.0625	0.0140	0.2005	0.7227	5.47

Table 1: Boundary conditions.

with oxygen and methane before being introduced into the McKenna burner. All lines between the vaporizer and the burner are heated to prevent GVL condensation. The exact mixture composition was measured at the burner exit in a cold configuration and is given in Table 1, in terms of mole fraction X_i.

2.1. Species measurements

An axially resolved species analysis was performed and 44 intermediate and product species are identified and quantified using gas chromatographs. All hydrocarbon and oxygenated species, water, and most permanent gases are analyzed using an Agilent 7890A gas chromatograph (GC) equipped with an HP-Plot Q column and a HP-Molsieve, a thermal conductivity detector (TCD), and a flame ionization detector (FID) with methanizer. The applied carrier gas is helium. A second GC, an HP 5890 gas chromatograph equipped with a carbosphere column and a TCD, is used for the quantification of hydrogen and oxygen. The utilization of argon as carrier gas allows for the quantification of oxygen without the need for separation of argon and oxygen in the column. The gas chromatographic measurements are calibrated using appropriate calibration gas mixtures. The detection limit of the FID is in the range of a few ppm for all relevant hydrocarbons, oxygenates, and carbon oxide species, whereas the detection limit for water, hydrogen, and oxygen is 50 ppm on the TCD. This results in an error of $\pm 5\%$ for the major species

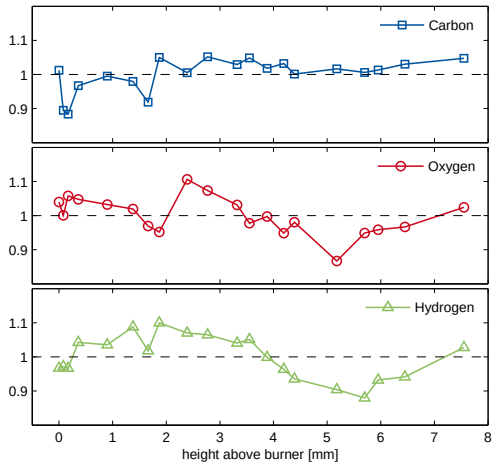

Figure 2: Carbon, oxygen, and hydrogen balance.

and ±10% for the minor species with mole fractions of less than 100 ppm (cf. [12]). The consistency of the species data is evaluated by calculating the sums of carbon, hydrogen, and oxygen atoms for all detected species at each height above the burner surface (HAB). The resulting carbon, hydrogen, and oxygen atom balances provided in Fig. 2 show, with the exception of single outliers, a carbon closure of ±5% and an oxygen and hydrogen closure of ±10%.

2.2. Flame temperature profiles

For the kinetic modeling of actual flames, the respective temperature profile of the flame is needed as input parameter to account for heat losses to the surroundings. Therefore, flame temperature measurements were performed using a 100 µm type B thermocouple with berillium oxide/yttrium oxide coating to prevent catalytic reactions, i.e. radical recombination at the thermocouple. The measurement point of the thermocouple is located at the tip of the probe for those measurements in which the probe is inserted into

the flame (cf. Fig. 1). At the high temperatures occurring in flames, radiative losses of the thermocouple are unavoidable and the recorded temperature is systematically lower than the actual flame temperature. Hence, the measured flame temperatures are corrected for the radiative heat losses applying correlations deducted through separate experiments using Joule heating of the thermocouple under vacuum [11]. The final uncertainty of the temperature measurements in the burned gas is ±100 K (cf. Ref. [12]). Additionally, the flame is disturbed to some extent by the quartz glass probe needed for the gas sampling. The probe has thus to be accounted for in the measurements and the temperatures are obtained with and without it being inserted into the flame. This yields an upper and a lower bound of the real flame temperature. The influence of the micro probe varies for different fuels and is found to be relatively large for the GVL/methane flame when compared to previously investigated flames (cf. Refs. [11, 12]). In Figure 3, the two measured temperature profiles are shown and it can be seen that although the shape of the profiles is similar, their axial location significantly differs. The temperature profiles are shifted along the HAB-axis to optimally depict the fuel decay under the assumption of independence of the species profiles from the flame location. This assumption has been been evaluated in form of a temperature profile sensitivity analysis of the calculated species profiles. The influence of the shifting on the maximum species concentrations was found to be within ±10% (±5% for all major species with the exception of CO_2). This is in the range of the species measurement uncertainties. Further, a good agreement prevails for the utilization of the different temperature profiles; cf. the supplementary material for details.

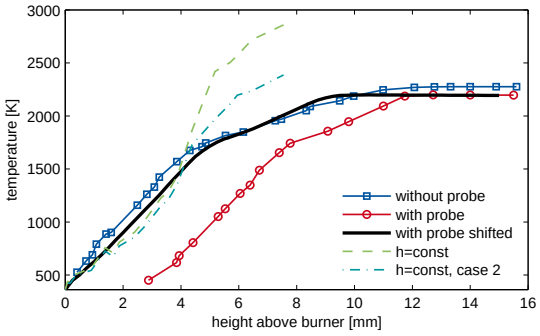

Figure 3: Temperature profiles of the GVL/methane flame.

In addition to the measured temperatures and the shifted temperature profile (with probe) used for all simulations, temperature profiles calculated as part of the enthalpy analysis are shown in Fig. 3. Preceding the discussion in Sec. 5, it shall be noted that a remarkable agreement between the temperature profile that follows from the thermodynamic analysis and the measured and shifted temperature profile exists for HABs $\leq$ 3.8 mm, which are obtained via two completely independent approaches.

3. Kinetic modeling

A kinetic model for the high temperature oxidation of GVL is proposed. The chemical structure of GVL is depicted in Fig. 4. Further shown are C-H bond dissociation energies (BDEs) and the carbon atom labeling used in the following. The BDEs show the significant influence that the ring oxygen and the carbonyl group exert on their neighboring C-H bonds, which has its origin in the stabilizing effects of radical delocalization from the oxygen moiety on radicals formed at the respective carbon sites.

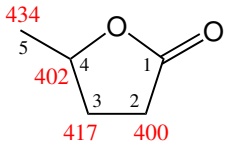

Figure 4: γ-valerolactone with atom labels (black) and C-H bond dissociation energies (red) in kJ/mol [8].

3.1. Model development

The GVL model consists of 346 species and 2854 reactions (forward and backward counted separately) and is based upon the C_0-C_4 mechanism of Blanquart et al. [13], it includes parts of the GVL pyrolysis model by De Bruycker et al. [9], and comprises a complementary sub-mechanism for the high-temperature oxidation of GVL. The C_0-C_4 base model has been extensively validated against ignition delay times, laminar burning velocities, and species profiles in various experimental setups [13] and has since been applied in a multitude of modeling studies [14–16]. The fuel specific reactions of the pyrolysis model of Ref. [9] are utilized in this study without modification, whereas the base mechanism of the pyrolysis model was replaced with the aforementioned model. In Ref. [9], the thermodynamic properties of species and kinetic data of reactions were determined with quantum chemical calculations at the CBS-QB3 level of theory. Calculated were among others the rate constants of GVL consumption including those of multiple radical/fuel hydrogen abstraction reactions and GVL isomerization to 4-pentenoic acid, some β-scission and isomerization reactions of the fuel radicals, and comparable reactions for the major pyrolysis intermediate 4-pentenoic acid. The complementary high temperature sub-model, developed as part of this work, describes the fuel specific combustion and is based on the concept of reaction

classes and rate rules [17, 18]. Major additions are the initiation reactions in oxidative environments, i.e. H-abstractions from the fuel and major intermediates by O_2, and H-abstraction reactions by O, OH, HO_2, and CH_3O_2 radicals. The rate coefficients for these reactions are prescribed assuming analogy to butanol using rate coefficients from Sarathy et al. [21], as the butanol rate coefficients consider the influence of oxygen on adjacent carbon atoms. The rate parameters for the isomerization reaction constants are determined based on analogies to the 2-methyltetrahydrofuran (2-MTHF) high temperature oxidation model by Moshammer et al. [19], as GVL's molecular structure is that of a 2-MTHF with an additional carbonyl group adjacent to the ring oxygen. Added were also oxidation reactions for the major pyrolysis product 4-pentenoic acid. The proposed model and the respective thermodynamic data are given in CHEMKIN format as supplementary material.

3.2. Flame simulations

1D unstretched burner-stabilized flame simulations were performed with the in-house developed FlameMaster code [20]. The source code is made available at http://www.itv.rwth-aachen.de/downloads/flamemaster. Calculations were performed for the boundary conditions given in Tab. 1. However, species measurements directly above the burner at 0.08 mm HAB show reduced GVL concentrations compared to the unburnt gas mixture. Further, certain levels of 1-butene, butadiene, propenal, 4-pentenoic acid, propene, ethylene, CO, and formaldehyde are detected. These species were all shown to be major pyrolysis products of GVL [9] and are hence assumed to result from GVL decomposition at the burner surface. To investigate the effect of the decomposition products on the GVL/methane flame, simulations with

(solid line plots) and without the decomposition products (dashed line plots) in the initial mixture are performed and shown in Fig. 5.

4. Results and discussion

Initially, the species measurements and model predictions are presented and discussed. Then, a reaction pathway analysis of GVL oxidation is performed with the proposed model.

4.1. Species measurement results and model performance

In Figure 5, the results of the species measurements and the flame simulations are given. It can be seen that small amounts of GVL are decomposed at the burner surface, but that the main GVL consumption occurs farther downstream, in the range of 2 to 4.4 mm HAB. Methane is available in the flame at slightly larger HABs and both fuel species are fully consumed at approximately 5 mm HAB. A very good agreement of the model and the experiment is achieved for the depletion of GVL and methane. Also, for the major intermediates and product species, a good agreement between model and experiment is found in the preheat and reaction zone of the flame, for HAB $<$ 4 mm. The model predicts CO_2 well until GVL is depleted and the H_2O concentration is in good agreement with the model until GVL and methane both are consumed. At larger HABs, the CO_2 and H_2O levels predicted by the model deviate from the measurements by 1-3.6 mol% for H_2O and by 2 mol% for CO_2. Some hydrogen (0.85 mol%) is detected directly at the burner surface. Subsequently, the hydrogen mole fraction increases at a relatively constant rate until its maximum of 2.6 mol% at 4.4 mm HAB

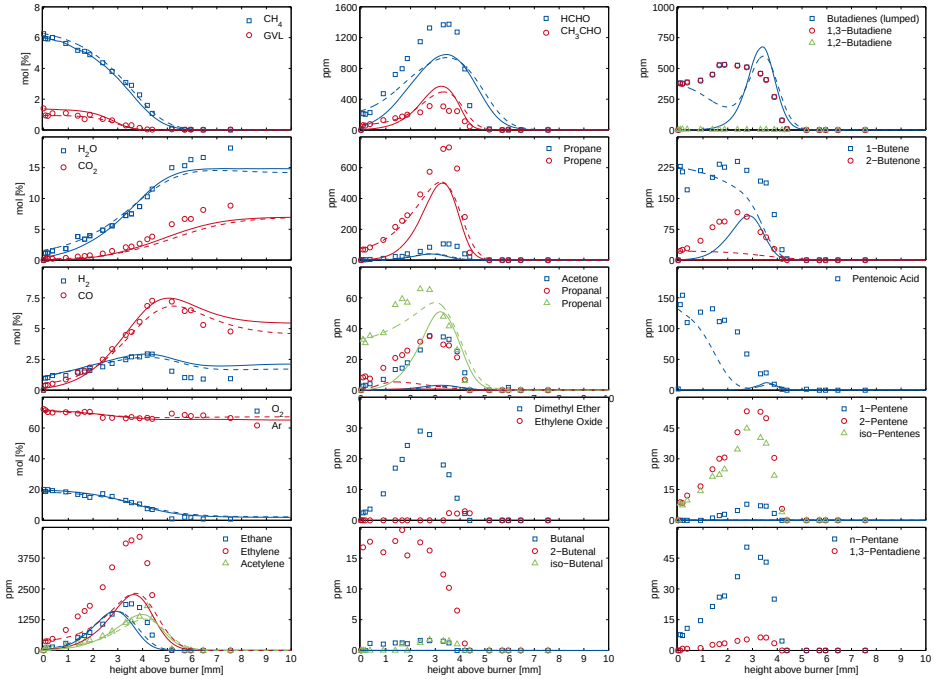

Figure 5: Mole fraction species evolution in the GVL/methane low pressure flame, (−) $T_{\mathrm{wProbe,shifted}}$; (−−) with decomposition, $T_{\mathrm{wProbe,shifted}}$.

is reached. Between 4.4 and 5.5 mm HAB, the hydrogen mole fraction decreases until it reaches a plateau of 0.82 mol% at about 6 mm HAB. The model captures the initial hydrogen production and the maximum concentration well, but the final hydrogen concentration is over-predicted by a factor of two. The CO mole fraction is matched well by the model until its peak concentration of 7.26 mol% is reached at 4.2 mm HAB. However, a deviation from model to experiment can be observed for larger HAB, at which the model prediction is lower than the experimental value. All larger hydrocarbon and oxygenated species are produced and consumed within the investigated low pressure flame. More precisely, they are fully consumed at an HAB of 4.4 mm. Generally, C_2 to C_5 alkanes, alkenes, dienes, ketones, and aldehydes were observed and most intermediates are reproduced well by the model, i.e. within a factor of two. The acetylene concentrations are almost perfectly matched and acetaldehyde is the only intermediate which is overpredicted by a factor of two. Most intermediates however are 10 to 50% underpredicted by the model. As the C_0 to C_4 base mechanism used in the GVL model lumps 1,3-butadiene and 1,2-butadiene, the experimental data are added and shown as butadienes, for which the maximum concentration is overpredicted by 50%. The isomer determination of the measurements yields the information, that 1,3-butadiene is dominating over 1,2-butadiene by orders of magnitude. Note also that butadiene is one of the main decomposition products of GVL. When considering the GVL decomposition products in the initial concentrations of the simulation, the species profiles are affected to a varying effect. These simulation results are shown as dashed lines in Fig. 5. According to the simulation, some of the intermediates, namely propanal, 2-

butenone, and 4-pentenoic acid, are almost entirely produced at the burner surface or origin from the combustion of one of the decomposition products, whereas others, such as 1-butene, butadiene, and propenal, are influenced to some extent by the decomposition but are genuine GVL combustion intermediates. The main intermediates, ethane, ethylene, acetylene, formaldehyde, acetaldehyde, propane, and propene are affected to a much lesser extent. For 1-butene, propenal, and propene, the species experimental data are better predicted when decomposition is taken into account. For butadiene, the influence is more specific. The model prediction with decomposition shows an initial decrease of the concentration of butadiene, before it is produced again in the flame. On the contrary, the species measurements show a small increase of the butadiene concentration between 0 to 4 mm HABs, before it is fully consumed at around 5 mm HAB. This indicates that early formation pathways for butadiene are missing in the model. Note further that 4-pentenoic acid and 1-butene are major products of GVL pyrolysis investigated by De Bruycker et al. [8]. In the flame modeling without decomposition, very low 4-pentenoic acid levels with a maximum of 7 ppm were predicted, which is much lower than its concentration in the measurements with a maximum of 150 ppm. In addition to the species shown in Fig. 5, further C_5 hydrocarbons and C_4 oxygenates were measured in minor amounts (<70 ppm) which are not included in the model. To be able to exclude fuel decomposition in the vaporizer, gas samples directly above the burner surface were taken without lighting of the flame. In this setup, only the fuel and the oxidizer species were detected. Hence, thermal cracking of the fuel in the vaporizer and heated lines prior to the burner can be excluded.

4.2. Reaction pathway analysis

An integrated reaction pathway analysis of GVL combustion was performed for the low pressure flame environment. The reaction pathways for the fuel oxidation are given in Fig. 6. It is shown to proceed mainly through H-abstraction by H radicals, but H-abstraction by O and isomerization to 4-pentenoic acid also contribute to the depletion of GVL. The most favored H-abstraction site is the tertiary C4 carbon atom (31%), followed by H-abstraction from C2 (20%), the carbon atom adjacent to the carbonyl group, from the C3 carbon atom (17%), and H-abstraction from the methyl side chain (11%). Fuel isomerization to 4-pentenoic acid, which is dominating GVL consumption in pyrolytic environments [9], is shown to contribute with 7% to the GVL depletion in this flame. Subsequently, the GVL radicals are consumed via ring-opening and β-scission, where C-O bond cleavage is favored over C-C bond cleavage. Merely for GVLR-4, which is stabilized through radical delocalization of the carbonyl group, isomerization pathways to different fuel radicals are of relevance. Important pathways for the ring opening products are decarbonylation and decarboxylation reactions where feasible, as well as C-C β-scission reactions. Stable species directly formed through the GVL oxidation pathways are acetaldehyde, ethylene, CO, and CO_2.

5. Enthalpy analysis

A complete species analysis, i.e. the quantification of all species in the flame gas sample, allows for an analysis of the flame enthalpy. As this is the case for the current GVL study, the consistency of the flame measurements

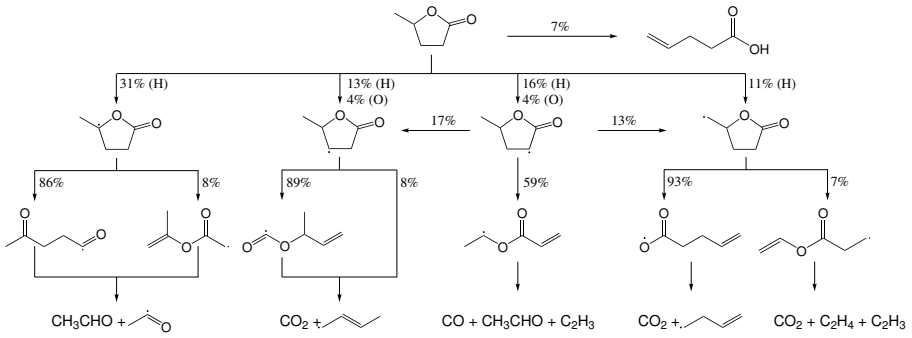

Figure 6: Reaction pathway analysis of GVL oxidation.

can be investigated in such terms. The total enthalpy in the flame, defined to include the species heat of formation and the thermal enthalpy is essentially constant in the flame according to the first law of thermodynamics. Downstram of the burner, it can only be modified by radiative heat loss and differential diffusion, where it should be noted that the latter cannot lead to an overall enthalpy loss, only to a redistribution. Both effects where found in numerical simulations for the present case to be negligibly small. The total enthalpy h is hence calculated according to

$$h = \sum_i h_i(T) Y_i = \text{const}, \tag{1}$$

where h_i denotes the specific enthalpy of a species i and Y_i its mass fraction. The contribution of each species is calculated using the species measurements and their specific enthalpies determined using the measured and shifted temperature profile at the respective HAB and evaluating the thermodynamic data available as part of the kinetic model. The total enthalpy is found to be approximately constant for HAB $\leq$ 3.8 mm, but significantly drops between 4 and 5 mm HAB, cf. Fig. 7. Considering the species concentrations at these

locations, the region of enthalpy loss coincides with the region in which the measured CO_2 and H_2O concentrations are higher and the CO, H_2, and O_2 concentrations are lower than those predicted by the model. Further, the oxygen and hydrogen balance show a decline of around 10% in this flame region. To elucidate the effect of the different $CO_2/H_2O/CO/H_2/O_2$ ratio, the enthalpy was reevaluated with the measured CO_2 and H_2O concentrations reduced while increasing H_2, CO, and O_2 according to $CO_2 \rightarrow CO + 1/2\ O_2$ and $H_2O \rightarrow H_2 + 1/2\ O_2$. For case 1, the two species were reduced such that all of the changed concentrations best match the model predictions. In this scenario, the H_2O level remains 1.5 mol% higher than predicted by the model. This is changed for case 2, in which the H_2O concentration is further reduced. The reduction of CO_2 and H_2O cuts the enthalpy loss by half. It is therefore concluded that the discrepancies between model and experiment at large HABs most likely originate from the experiment at large HABs and not from the proposed model. Even though the hydrogen and oxygen atom balance decrease in this temperature range, it is approximately unity for the largest HAB, at which the total enthalpy is still reduced compared to the smaller HABs. Hence, the hydrogen and oxygen atom balance are not the reason for the enthalpy loss. In a second step, the flame temperature is calculated solely based on the species measurements under the assumption of total enthalpy conservation throughout the flame. The initial enthalpy (unburnt species mixture, burner temperature) is assumed to prevail at all HABs. Thereby, the temperature at each gas sampling location is calculated iteratively from the measured species concentrations using eq. (1). The calculated temperature for the measurements and case 2 are shown in Fig. 3 in

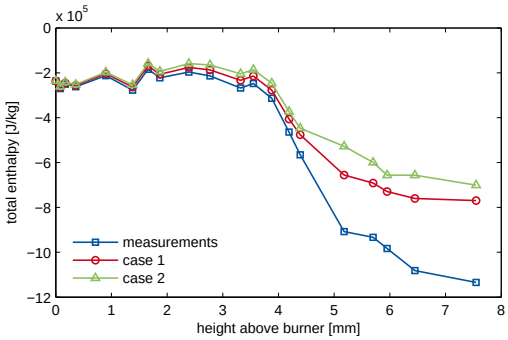

Figure 7: Total enthalpy at each HAB.

addition to the measured temperature profiles. In correspondence to the loss of total enthalpy depicted in Fig. 7, the agreement of the calculated and the shifted temperature profile is very good for HABs of up to 3.8 mm. As the temperature calculation from enthalpy is independent of the experimentally obtained temperature profiles, this agreement shows the high consistency of the two data sets obtained with two completely different measurement techniques. However, this also indicates experimental issues at larger HABs. The good agreement of the measured and the calculated temperature profile in regions with constant enthalpy further suggests that calculating the temperature from the species measurement can be a valid option to obtain the temperature profile in a low pressure flame, if it can be ensured that the species measurements are complete and correct.

6. Conclusions

The first fundamental experimental and modeling study of the oxidation of GVL was performed and species profiles for oxygen, hydrogen, argon, carbon monoxide, carbon dioxide, water, and hydrocarbon species, including

oxygenated species and separated isomers, were presented. Typical intermediate species occurring in flames, e.g. hydrocarbons and oxygenates with carbon numbers of one and two, were measured. High mole fractions of ethane, ethylene, and acetylene in the range of 2000 to 4000 ppm were found. A kinetic model for the pyrolysis of GVL was extended for combustion modeling and the model predictions showed a good agreement with the species data in the preheat and reaction zone of the flame until the fuel is depleted. For larger HABs, deviations between the model and the measurements occurred. A thermodynamic analysis of the flame was performed from which a flame temperature solely based on the species measurements was calculated. This temperature agrees very well with the measured and shifted temperature profile used for the simulations in the preheat and reaction zone of the flame up to the point where the fuel is depleted. Thereby, the consistency of two independent measurement techniques applied in the flame is shown which builds confidence in the experimental data set. On the contrary, the analysis also identified parts of the species measurements that have to be handled with care. In the regions of high HABs, CO_2 and H_2O were significantly larger and H_2, O_2, and CO smaller compared to the simulation. The enthalpy analysis suggests that this discrepancy is due to the measurements and not to the model. As this additional information is of high value, especially for future modeling work, it is strongly encouraged to perform corresponding enthalpy analyses alongside any future low pressure flat flame study.

Acknowledgements

This work was funded by the Cluster of Excellence "Tailor-Made Fuels from Biomass", which is funded by the Excellence Initiative by the German federal and state governments to promote science and research at German universities.

[1] I. T. Horváth, H. Mehdi, V. Fábos, L. Boda and L. T. Mika, Green Chemistry 10 (2008) 238-242.

[2] X. Tang, X. Zeng, Z. Li, L. Hu, Y. Sun, S. Liu, T. Lei, L. Lin, Renew. Sust. Energ. Rev. 40 (2014) 608-620.

[3] K. Yan, T. Lafleur, C. Jarvis, G. Wu, J. Clean. Prod. 72 (2014) 230-232.

[4] Á. Bereczky, K. Lukács, M. Farkas, S. Dóbé, Nat. Resour. J. 5 (2014) 177-191.

[5] A. M. Raspolli Galletti, C. Antonetti, E. Ribechini, M. P. Colombini, N. Nassio Di Nasso, E. Bonari, Appl. Energ. 102 (2013) 157-162.

[6] S. G. Wettstein, D. M. Alonso, Y. Chong, J. A. Dumesic, Energy Environ. Sci. 5 (2012) 8199-8203.

[7] X. Tang, H. Chen, L. Hu, W. Hao, Y. Sun, X. Zeng, L. Lin, S. Liu, Appl. Catal. B 147 (2014) 827-834.

[8] R. De Bruycker, H.-H. Carstensen, J. M. Simmie, K. M. Van Geem, G. B. Marin, Proc. Combust. Inst. 35 (2015) 515-523.

[9] R. De Bruycker, H.-H. Carstensen, M.-F. Reyniers, G. B. Marin, J. M. Simmie, K. M. Van Geem, *accepted for publication at* Combust. Flame.

[10] L. S. Tran, C. Togbé, D. Liu, D. Felsmann, P. Oßwald, P.-A. Glaude, R. Fournet, B. Sirjean, F. Battin-Leclerc, K. Kohse-Höinghaus, Combust. Flame 161 (3) (2014) 766-779.

[11] L. S. Tran (2013), *Etude de la formation de polluants lors de la combustion de carburants oxygénés*, Ph.D. Thesis, Université de Lorraine, France, `http://docnum.univ-lorraine.fr/public/DDOC_T_2013_0171_TRAN.pdf`.

[12] L. S. Tran, P.-A. Glaude, R. Fournet, F. Battin-Leclerc, Energy Fuels 27 (2013) 2226-2245.

[13] G. Blanquart, P. Pepiot-Desjardins, H. Pitsch, Combust. Flame 156 (3) (2009) 588-607.

[14] K. Narayanaswamy, G. Blanquart, H. Pitsch, Combust. Flame 157 (10) (2010) 1879-1898.

[15] K. Narayanaswamy, P. Pepiot, H. Pitsch, Combust. Flame 161(4) (2014) 866-884.

[16] L. Cai, Y. Uygun, C. Togbé, H. Pitsch, H. Olivier, P. Dagaut, S. M. Sarathy, Proc. Combust. Inst. 35 (2015) 419-427.

[17] S. M. Sarathy, C. K. Westbrook, M. Mehl, W. J. Pitz, C. Togbé, P. Dagaut, H. Wang, M. A. Oehlschlaeger, U. Niemann, K. Seshadri, P.

S. Veloo, C. Ji, F. N. Egolfopoulos, T. Lu, Combust. Flame 158 (12) (2011) 2338-2357.

[18] H. J. Curran, P. Gaffuri, W. J. Pitz, C. K. Westbrook, Combust. Flame 144 (1) (1998) 149-177.

[19] K. Moshammer, S. Vranckx, H. K. Chakravarty, P. Parab, R. X. Fernandes, K. Kohse-Höinghaus, Combust. Flame 160 (12) (2013) 2729-2743.

[20] H. Pitsch, FlameMaster: A C++ computer program for 0D combustion and 1D laminar flame calculations, 1993.

[21] S. M. Sarathy, S. Vranckx, K. Yasunaga, M. Mehl, P. Oßwald, W. K. Metcalfe, C. K. Westbrook, W. J. Pitz, K. Kohse-Höinghaus, R. X. Fernandes and others, Comb. Flame 159 (6) (2012) 2028-2055.